Magnetic penetration depth and T_c in superconducting nickelates

F. Bernardini,[1] V. Olevano,[2] and A. Cano[2]
[1]*Dipartimento di Fisica, Università di Cagliari, IT-09042 Monserrato, Italy*
[2]*CNRS & UGA, Institut Néel, 38042 Grenoble, France*

(Received 30 October 2019; revised manuscript received 21 January 2020; accepted 4 February 2020; published 27 February 2020)

We compute the nominal magnetic penetration depth of $R\mathrm{NiO_2}$ (R = La, Nd) from first-principles calculations and discuss the results in relation to the superconducting T_c. We find a marked discrepancy with the well-established phenomenology that correlates these two quantities in cuprates (Uemura plot). We also consider the two-dimensional ultrathin limit and estimate the maximum attainable T_c to be ∼180 K according to the Nelson-Kosterliz universal relation between the superfluid density and the transition temperature.

DOI: 10.1103/PhysRevResearch.2.013219

I. INTRODUCTION

The recent discovery of superconductivity in Sr-doped $\mathrm{NdNiO_2/SrTiO_3}$ thin films [1] has attracted an instantaneous research attention (see, e.g., [2–13]). After many attempts, this can potentially be the first successful extension of high-T_c cuprate superconductivity to isostructural/isoelectronic nickelates. This important breakthrough can thus shed light on their elusive microscopic superconducting mechanism, even if it poses some important challenges to current paradigms. In particular, the parent nickelates are metals without magnetic order as opposed to their cuprate counterparts that are antiferromagnetic charge-transfer insulators. Consequently, Cooper pairing in (Nd,Sr)$\mathrm{NiO_2}$ seems to emerge from a rather different normal nonsuperconducting state.

First-principles calculations based on density-functional theory (DFT) consistently find that, among the five Ni-3d bands, only the $3d_{x^2-y^2}$ states intercept the Fermi level [2–6,14]. This establishes a promising analogy to $\mathrm{CaCuO_2}$, i.e., the parent compound of high-T_c cuprates. In fact, the electron-phonon coupling has been ruled out as the exclusive origin of the observed superconductivity in (Nd,Sr)$\mathrm{NiO_2}$ [5]. At the same time, electrons in the Nd layer make additional electron pockets in the Fermi surface that likely prevent the system from being a simple Mott insulator, with Kondo physics potentially playing a role [6–8]. Besides, the charge-transfer gap between the Ni-3d states and O-2p states is larger than that in cuprates [9]. On the other hand, spin fluctuations may still be important for superconductivity, even if there is no long-range magnetic order. In that case, the dominant pairing has been proposed to yield a d-wave superconducting gap [3,4] with a distinct spin resonance feature that can be tested experimentally [10]. Here, we compute the nominal magnetic penetration depth of the superconducting nickelates as a function of hole doping and discuss these theoretical results in relation to the observed T_c.

II. PRELIMINARIES

A. Zero-temperature magnetic penetration depth as a band-structure property

The magnetic penetration depth λ is pivotal to explain the Meissner effect and therefore is a fundamental quantity of superconductors [15]. This quantity can be determined experimentally by means of different complementary techniques such as the tunnel diode oscillator technique [16,17] and muon-spin resonance (μSR) [18–21]. The temperature dependence of λ maps the amount of excited quasiparticles and thereby the structure of the superconducting gap. However, in the London approximation, the zero-temperature magnetic penetration depth in the clean limit reduces to $\lambda_L(T=0) = \sqrt{\frac{m^*}{\mu_0 n_s e^{*2}}}$, where m^* is the effective mass of charge carriers, μ_0 is the vacuum permeability, n_s is the charge carrier density, and e^* is an effective electron charge. Thus, it basically becomes a band-structure property formally unrelated to the gap function. In fact, from a semiclassical generalization of the London equation [22] or Eilenberger's formulation of superconductivity [23] (see Appendix A), a band-structure-specific result can be obtained as

$$(\lambda^2)^{-1}_{ij}(T=0) = \frac{\mu_0 e^2}{4\pi^3\hbar}\oint_{\mathrm{FS}} dS \frac{v_{Fi}v_{Fj}}{v_F}, \tag{1}$$

where the integral is over the Fermi surface with $\mathbf{v}_F$ being the Fermi velocity (the subscripts $i, j = x, y, z$ refer to principal axes). In the following, we will make use of this result to discuss the superconducting properties of the nickelates.

B. Computational methods

We computed Eq. (1) from DFT calculations that conveniently reproduce the reported band structure of the La and Nd nickelates. Specifically, we used the FLAPW method as

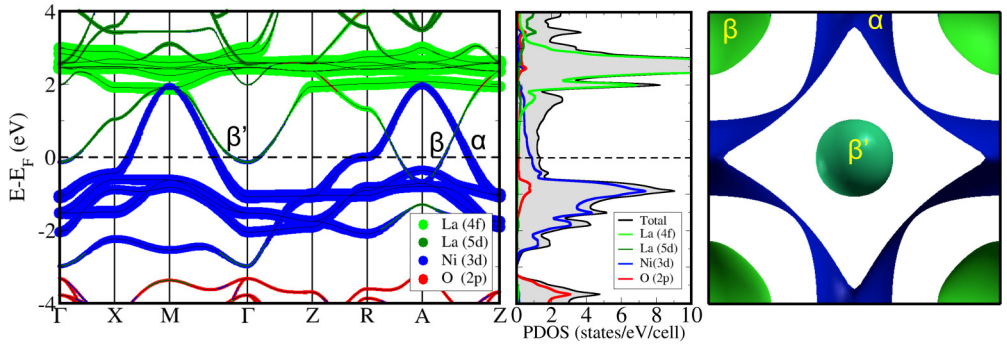

FIG. 1. First-principles band structure (left, "fatband" plot), orbital resolved density of states (middle), and top view of Fermi surface (right) of $LaNiO_2$.

implemented in the WIEN2K package [24] with the local density approximation (LDA) exchange-correlation functional [25]. In order to avoid the ambiguous treatment of the f-orbital bands, we followed [2,3] and focused on the mother compound $LaNiO_2$. Further, we modeled Sr doping as a rigid shift of the Fermi level as in [4] and also within the virtual-crystal approximation (VCA) as in [3]. We also considered $NdNiO_2$ with the Nd-4f states in the core as well as the influence of epitaxial strain, with which we obtained almost identical results. We performed spinless calculations with muffin-tin radii of 2.5, 2.1, and 1.62 a.u. for the La (Nd), Ni, and O atoms, respectively, and a plane-wave cutoff $R_{\mathrm{MT}}K_{\max} = 7.0$. The integration over the Brillouin zone was performed using a $11 \times 11 \times 14\,k$ mesh for the self-consistent calculations, while a dense $48 \times 48 \times 48\,k$ mesh was used to compute and study the Fermi surface. In our calculations, the Fermi velocity is directly obtained from the expectation value of the momentum operator $\mathbf{p}$ ($\mathbf{v}_F = \mathbf{p}_F/m$), and the dense k mesh was used to further perform the Fermi-surface integral.

III. RESULTS

Figure 1 illustrates the reference band structure of the infinite-layer nickelates [2–4,14,27]. The Ni-3d states intercepting the Fermi level give rise to the large holelike Fermi surface α dominated by $3d_{x^2-y^2}$ contributions. Interestingly, this pocket α seems to originate from two different bands that undergo an avoided crossing along the Z-R path where their $d_{x^2-y^2}$ and d_{z^2} characters swap (see Appendix B). To the best of our knowledge, this feature was first pointed out in [28]. We find that this avoided crossing and its concomitant $d_{x^2-y^2}$-d_{z^2} mix changes with doping (see Appendix B), thereby having a potential effect on the superconducting instability [29] that has not been considered so far. In addition, there is a self-doping effect due to La-5d states that results into to the extra electronlike Fermi surfaces β and β'.

The nominal $\lambda(0)$ of the superconducting nickelates as a function of Sr doping is reported in Table I. These values are obtained using a rigid shift of the Fermi level, and essentially the same is obtained using VCA (see Appendix C). Even if superconductivity has been reported for 20% doping so far, the nominal values computed for other dopings allow us to get an idea of the possible variations in $\lambda(0)$ due to physical changes in the corresponding band structure (which can be taken as a sort of "error bar"). These results confirm that (Nd,Sr)NiO_2 is a type-II superconductor (i.e., $\kappa \equiv \lambda/\xi > 1/\sqrt{2}$, with $\xi = 3.25$ nm being the Ginzburg-Landau coherence length [1]). In the case of the overall in-plane component $\lambda_x(0)$, the main contribution originates from the main hole pocket α and does not vary dramatically with doping. The out-of-plane component $\lambda_z(0)$, in contrast, is initially dominated by the electron pocket β and therefore undergoes a more substantial change as β shrinks with doping. Note that, despite the apparent two-dimensional (2D) character of α [14], the anisotropy of this contribution is moderate compared to that in

TABLE I. Zero-temperature magnetic penetration length obtained from DFT calculations in the London approximation for different values of Sr (hole) doping (modeled as a rigid shift of the Fermi level). Only the diagonal terms are nonzero by symmetry, and are denoted by a single subscript ($\lambda_x = \lambda_y$ and λ_z). The effective lambda is defined as $\lambda_{\mathrm{eff}} = 3^{1/4}[1 + 2(\lambda_x/\lambda_z)^2]^{-1/4}\lambda_x$, as probed by μSR in polycrystalline samples [26]. The values for $NdNiO_2$ are obtained assuming the Nd-4f states in the core.

	Doping	FS	$(\lambda_x(0), \lambda_z(0))$ (nm)	$\lambda_{\mathrm{eff}}(0)$ (nm)
$LaNiO_2$	0	α	(47, 245)	61
		β	(140, 120)	133
		β'	(365, 300)	340
		Total	(44, 101)	54
	0.1	α	(49, 170)	62
		β	(165, 140)	156
		Total	(47, 108)	57
	0.2	α	(50, 215)	64
		β	(205, 175)	194
		Total	(48, 136)	60
	0.3	α	(51, 160)	64
		β	(275, 240)	262
		Total	(50, 133)	62
	0.4	α	(54, 163)	68
		β	(450, 580)	486
		Total	(54, 156)	67
$NdNiO_2$	0.2	α	(49, 180)	62
		β	(190, 160)	179
		β'	(290, 220)	262
		Total	(47, 105)	57

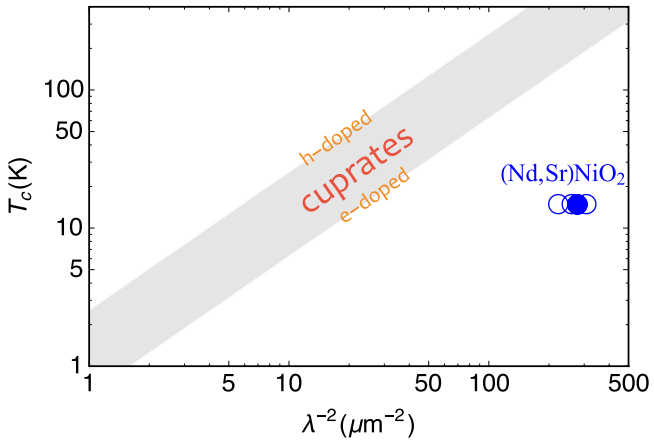

FIG. 2. Uemura log-log plot for the zero-temperature effective magnetic penetration depth of (Nd,Sr)NiO_2 computed from Eq. (1). The solid circle corresponds to 20% Sr doping and $T_c = 15$ K, while the open circles are associated to the 10%, 30%, and 40% dopings in Table I assuming the same T_c.

cuprates and displays a nonmonotonous behavior with doping. This should not be surprising if the α pocket results from two different bands undergoing an avoided crossing that changes with doping (see Fig. 3 in Appendix B). Beyond that, the effective λ_{eff} probed by μSR turns out to be essentially that of the hole pocket α (with β having the effect of reducing the anisotropy resulting from α only).

IV. DISCUSSION

Our results are summarized in Fig. 2 in a Uemura plot. As we can see, the calculated λ_{eff}'s are totally off the expected values for a cuprate with $T_c \approx 15$ K (shaded region). The modification of the effective mass due to correlations can to some extent improve the agreement. However, the mass has to be >10 times larger to do the job, which seems unlikely according to DMFT results (see, e.g. [13]).

We note that a presumably related discrepancy has been pointed out for the Hall resistance of the parent compound [2]. Specifically, the Hall coefficient is inconsistent with the large holelike Fermi surface α. To reproduce the sign of the measured coefficient and obtain a fair agreement with its numerical value, a gapped α pocket has to be assumed. Analogously, in the case of the magnetic penetration depth, the cuprate trend in the Uemura plot is regained if the α contribution is neglected and only the electron pocket β is taken account for $\lambda(0)$ at 20% Sr doping. Even if the Hall coefficient and $\lambda(0)$ are both a measure of the DOS, one would tend to think that is rather fortuitous coincidence. In any case, this illustrates that reconciling these estimates with the well-established phenomenology of cuprates seems to require a rather significant modification of the corresponding band structure (this, or the system is to be understood as a failed room-temperature superconductor according to its λ).

Alternatively, superconductivity in (Nd,Sr)NiO_2 thin films can be a 2D phenomenon and hence a different rationale must be applied. This will be naturally the case in the ultrathin limit, and will also be relevant if superconductivity is eventually driven by the interface with the substrate [30,31]. The magnetic penetration depth, being a measure of the superfluid density, is also related to the superfluid stiffness D_s. This relation can be exploited to set bounds on the superconducting transition temperature since fluctuations of the phase of the superconducting order parameter will be the ultimate limiting factor in 2D [32]. Such a bound directly reads from Nelson-Kosterlitz universal jump of the superfluid density [33]:

$$k_B T_c \leqslant \pi D_s/2. \tag{2}$$

The 2D superfluid stifness can be estimated from our previous calculations as $D_s \approx \frac{\hbar^2}{4\mu_0 e^2}\frac{d}{2\pi}\lambda_x^{-2}$, where d is the interlayer spacing (i.e., the c lattice parameter). This gives a maximum T_c of about 145 K. By restricting the integral (1) to the $k_{Fz} = 0$ line of the three-dimensional (3D) Fermi surface this value increases to 180 K. While formally rigorous, this estimate has to be understood as a rather conservative upper bound since the superfluid density at $T = 0$, and hence the corresponding stiffness, can reasonably be assumed to overestimate that at T_c.

V. CONCLUSIONS

In summary, we have computed the zero-temperature magnetic penetration depth $\lambda(0)$ of the newly superconducting nickelate $NdNiO_2$ relying on first-principles DFT calculations to fully take into account its band-structure specific features. $\lambda(0)$ is a fundamental descriptor of superconductivity displaying a phenomenological correlation to T_c in cuprates and in other unconventional superconductors. Our calculations confirm the system as a type-II superconductor. The in-plane component of $\lambda(0)$ is found to be dominated by the hole Fermi-surface pocket and no substantial change is obtained with doping. However, the extra electron pocket has a non-negligible impact on the eventual anisotropy. Remarkably, the nominal $\lambda(0)$ and the reported T_c do not follow the same correlation observed in the cuprates. If the same correlation were to apply, $NdNiO_2$ would be a room-temperature superconductor. This suggests that either the reported band structure needs to be revisited or the superconducting nature of nickelates is different. In the 2D case relevant for the ultrathin limit and/or if the actual phenomenon corresponds to interfacial superconductivity [30,31], the maximum attainable T_c is estimated to be ∼180 K from the Nelson-Kosterlitz universal jump of the superfluid density.

ACKNOWLEDGMENT

F.B. acknowledges the Visiting Scientist Program of the Centre de Physique Theorique de Grenoble-Alpes (CPTGA) for financial support.

APPENDIX A: DERIVATION OF EQ. (1).

Here, we outline the derivation of Eq. (1) within Eilenberger's formulation of superconductivity. This derivation can be found in more detail in [17,23], for example. Eilenberger's picture is obtained directly from Gor'kov equations after integrating out fast-varying degrees of freedom [34]. Thus, the

current density reads as

$$\mathbf{j} = -4\pi e k_B T \ \mathrm{Im} \sum_{\omega>0} \langle \mathbf{v}_F g \rangle, \tag{A1}$$

where g is the Eilenberger function associated to normal excitations. Here, $\omega = (2n+1)\pi k_B T/\hbar$ are Matsubara frequencies and the average is defined such that $\langle X \rangle = \int \frac{d^2 k_F}{(2\pi)^3 \hbar v_F} X$. In the clean case, Eq. (A1) for the current is supplemented by the set of equations

$$(\hbar \mathbf{v}_F \cdot \mathbf{\Pi} + 2\hbar\omega) f = 2\Delta g, \tag{A2}$$

$$(-\hbar \mathbf{v}_F \cdot \mathbf{\Pi}^* + 2\hbar\omega) f^+ = 2\Delta^* g, \tag{A3}$$

$$\Delta(\mathbf{r}, \mathbf{v}_F) = 2\pi k_B T \sum_{\omega>0}^{\omega_{\max}} \langle V(\mathbf{v}_F, \mathbf{v}'_F) f(\mathbf{r}, \omega, \mathbf{v}'_F) \rangle_{\mathbf{v}'_F}, \tag{A4}$$

where $\mathbf{\Pi} = \nabla - \frac{2ie}{\hbar}\mathbf{A}$. Here Δ and V represent the gap function and the effective coupling, respectively, while the functions f and f^+ describe the superconducting condensate and are such that $f f^+ = 1 - g^2$. In the absence of currents and fields, the ground-state uniform solution of Eilenberger equations reads as $f_0 = f_0^+ = \Delta_0/(\Delta_0^2 + \hbar^2\omega^2)^{1/2}$, $g_0 = \hbar\omega/(\Delta_0^2 + \hbar^2\omega^2)^{1/2}$. The presence of weak fields and supercurrents can be treated perturbatively to obtain $g = g_0 + g_1$, where the correction g_1 reads as $g_1 = i\hbar \frac{\Delta_0^2}{2(\Delta_0^2+\hbar^2\omega^2)^{3/2}} \mathbf{v}_F \cdot (\nabla\theta + \frac{2e}{\hbar}\mathbf{A})$, with θ being the overall phase acquired by Δ, f, and f^+. Substituting this in Eq. (1) yields the London relation $j_i = -\frac{1}{\mu_0}(\lambda^2)^{-1}_{ij} a_j$ between the current and the "gauge-invariant vector potential" $\mathbf{a} = \frac{\hbar}{2e}\nabla\theta + \mathbf{A}$, where

$$(\lambda^2)^{-1}_{ij} = 4\pi\mu_0 e^2 k_B T \sum_{\omega>0} \left\langle \frac{\Delta_0^2 v_{Fi} v_{Fj}}{\left(\Delta_0^2 + \hbar^2\omega^2\right)^{3/2}} \right\rangle. \tag{A5}$$

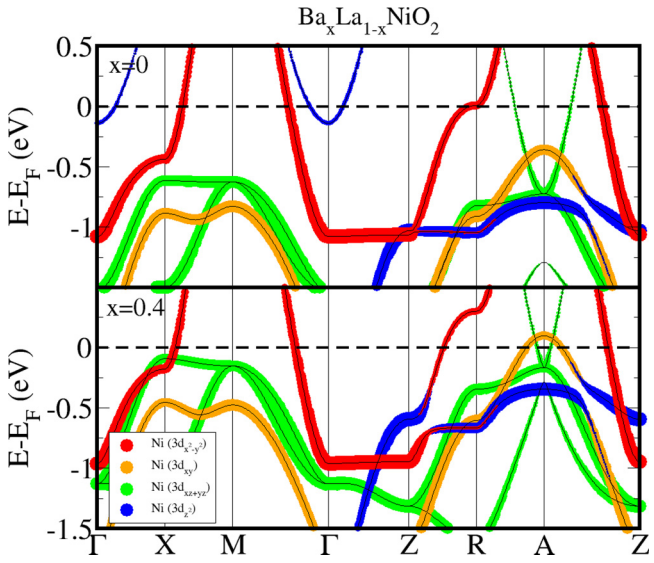

FIG. 3. Zoom of the electronic band structure of $LaNiO_2$ (top) and $La_{0.6}Ba_{0.4}NiO_2$ within VCA (bottom) in a "fatband" plot.

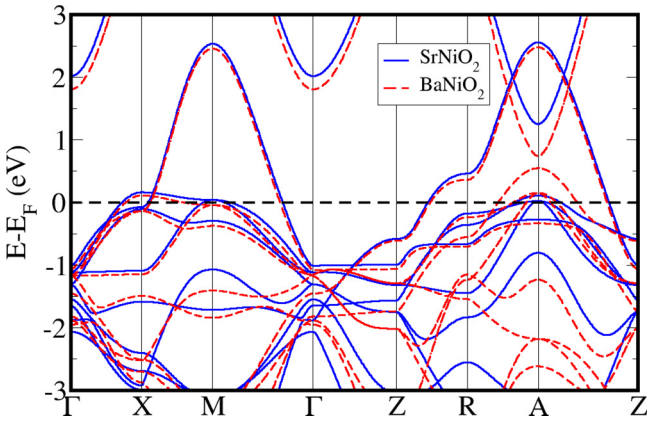

FIG. 4. Band structure of $SrNiO_2$ and $BaNiO_2$ compared.

In the $T = 0$ limit,

$$\begin{aligned}(\lambda^2)^{-1}_{ij}(T=0) &= 2\mu_0 e^2 \hbar \left\langle v_{Fi} v_{Fj} \int_0^\infty d\omega \frac{\Delta_0^2}{\left(\Delta_0^2 + \hbar^2\omega^2\right)^{3/2}} \right\rangle \\ &= 2\mu_0 e^2 \hbar \left\langle v_{Fi} v_{Fj} \frac{\omega}{\left(\Delta_0^2 + \hbar^2\omega^2\right)^{1/2}} \Big|_0^\infty \right\rangle \\ &= 2\mu_0 e^2 \langle v_{Fi} v_{Fj} \rangle, \end{aligned} \tag{A6}$$

which corresponds to Eq. (1).

APPENDIX B: AVOIDED CROSSING AND $d_{x^2-y^2}$-d_{z^2} MIX

Figure 3 shows a zoom of the electronic band structure of (La,Ba)NiO_2 near the Fermi level. As we can see, the Ni-3d states generating the holelike pocket in the Fermi surface (α in Fig. 1) appears to be associated to two different bands. These bands undergo an avoided crossing along the Z-R path that changes with doping. Thus, the apparent 2D α pocket is in reality a 3D one by its very nature.

TABLE II. Zero-temperature magnetic penetration length obtained from DFT calculations in the London approximation for different values of Ba (hole) doping (modeled using the VCA). The effective lambda is defined as $\lambda_{\mathrm{eff}} = 3^{1/4}[1 + 2(\lambda_x/\lambda_z)^2]^{-1/4}\lambda_x$, as probed by μSR in polycrystalline samples [26].

$La_{1-x}Ba_xNiO_2$	FS	$(\lambda_x(0), \lambda_z(0))$ (nm)	$\lambda_{\mathrm{eff}}(0)$ (nm)
$x = 0.1$	α	(49, 168)	62
	β	(164, 145)	157
	Total	(47, 110)	57
$x = 0.2$	α	(50, 153)	63
	β	(210, 197)	205
	Total	(49, 121)	60
$x = 0.3$	α	(51, 156)	64
	β	(284, 285)	284
	Total	(50, 138)	62
$x = 0.4$	α	(52, 163)	65
	β	(345, 400)	361
	Total	(52, 151)	65

APPENDIX C: VCA CALCULATIONS

Here, we report additional calculations using the virtual-crystal approximation (VCA) and comment on this approach for the infinite-layer nickelates. We restrict ourselves to the mother compound $LaNiO_2$ and consider the substitution of La with Ba instead of Sr as in [3]. Thus, we consider the $La_{1-x}Ba_xNiO_2$ material which is further modeled by a virtual compund $XNiO_2$ where the X atom has a nuclear charge $Z = 57 - x$. We note that this strategy would be perfect if the band structure of $SrNiO_2$ and $BaNiO_2$ were identical. However, this is not exactly the case as can be seen in Fig. 4. In particular, the dispersion of the bands is noticeably different at the A point which leads to non-negligible differences in the Fermi surface. This will be more important for the case of electron doping. Despite of such a difference, the values of $\lambda(0)$ calculated using the VCA are essentially the same as those calculated with the rigid band approximation (see Table II). In addition, the two methods yield the exactly same trend as a function of doping: while both λ_x and the β contribution to λ_z increase with doping, the α contribution to λ_z displays a nonmonotonous behavior. The agreement obtained using these two different approaches thus strengthens the validity of our results.

[1] D. Li, K. Lee, B. Y. Wang, M. Osada, S. Crossley, H. R. Lee, Y. Cui, Y. Hikita, and H. Y. Hwang, Nature (London) **572**, 624 (2019).

[2] A. S. Botana and M. R. Norman, Phys. Rev. X **10**, 011024 (2020).

[3] H. Sakakibara, H. Usui, K. Suzuki, T. Kotani, H. Aoki, and K. Kuroki, arXiv:1909.00060.

[4] X. Wu, D. D. Sante, T. Schwemmer, W. Hanke, H. Y. Hwang, S. Raghu, and R. Thomale, arXiv:1909.03015.

[5] Y. Nomura, M. Hirayama, T. Tadano, Y. Yoshimoto, K. Nakamura, and R. Arita, Phys. Rev. B **100**, 205138 (2019).

[6] M. Hepting *et al.*, Nat. Mater. (to be published) (2020), doi: 10.1038/s41563-019-0585-z.

[7] G.-M. Zhang, Y.-F. Yang, and F.-C. Zhang, Phys. Rev. B **101**, 020501 (2020).

[8] Y.-H. Zhang and A. Vishwanath, arXiv:1909.12865.

[9] M. Jiang, M. Berciu, and G. A. Sawatzky, arXiv:1909.02557.

[10] T. Zhou, Y. Gao, and Z. D. Wang, arXiv:1910.05757.

[11] J. E. Hirsch and F. Marsiglio, Physica C (Amsterdam) **566**, 1353534 (2019).

[12] L.-H. Hu and C. Wu, Phys. Rev. Research **1**, 032046 (2019).

[13] S. Ryee, H. Yoon, T. J. Kim, M. Y. Jeong, and M. J. Han, arXiv:1909.05824.

[14] K.-W. Lee and W. E. Pickett, Phys. Rev. B **70**, 165109 (2004).

[15] M. Tinkham, *Introduction to Superconductivity* (Dover, New York, 2004).

[16] R. Prozorov and R. W. Giannetta, Supercond. Sci. Technol. **19**, R41 (2006).

[17] R. Prozorov and V. G. Kogan, Rep. Prog. Phys. **74**, 124505 (2011).

[18] Y. J. Uemura, G. M. Luke, B. J. Sternlieb, J. H. Brewer, J. F. Carolan, W. N. Hardy, R. Kadono, J. R. Kempton, R. F. Kiefl, S. R. Kreitzman *et al.*, Phys. Rev. Lett. **62**, 2317 (1989).

[19] A. Amato, Rev. Mod. Phys. **69**, 1119 (1997).

[20] J. E. Sonier, J. H. Brewer, and R. F. Kiefl, Rev. Mod. Phys. **72**, 769 (2000).

[21] A. Bhattacharyya, D. T. Adroja, M. Smidman, and V. K. Anand, Sci. China: Phys., Mech. Astron. **61**, 127402 (2018).

[22] B. S. Chandrasekhar and D. Einzel, Ann. Phys. **505**, 535 (1993).

[23] V. G. Kogan, Phys. Rev. B **66**, 020509(R) (2002).

[24] P. Blaha, K. Schwarz, G. Madsen, D. Kvasnicka, J. Luitz, R. Laskowski, F. Tran, and L. D. Marks, WIEN2k, An Augmented Plane Wave + Local Orbitals Program for Calculating Crystal Properties (Karlheinz Schwarz, Techn. Universität Wien, Austria, 2018).

[25] J. P. Perdew and A. Zunger, Phys. Rev. B **23**, 5048 (1981).

[26] V. Fesenko, V. Gorbunov, and V. Smilga, Physica C (Amsterdam) **176**, 551 (1991).

[27] V. I. Anisimov, D. Bukhvalov, and T. M. Rice, Phys. Rev. B **59**, 7901 (1999).

[28] F. Bernardini, V. Olevano, X. Blase, and A. Cano, arXiv:1911.11788.

[29] H. Sakakibara, H. Usui, K. Kuroki, R. Arita, and H. Aoki, Phys. Rev. B **85**, 064501 (2012).

[30] Q. Li, C. He, J. Si, X. Zhu, Y. Zhang, and H.-H. Wen, arXiv:1911.02420.

[31] F. Bernardini and A. Cano, arXiv:2001.02133.

[32] T. Hazra, N. Verma, and M. Randeria, Phys. Rev. X **9**, 031049 (2019).

[33] D. R. Nelson and J. M. Kosterlitz, Phys. Rev. Lett. **39**, 1201 (1977).

[34] G. Eilenberger, Z. Phys. A **214**, 195 (1968).